Supplementary Information (SI) for RSC Advances.

Supporting information

Tunable Dispersion of Cobalt Oxide Nanoclusters Grafted on Mesoporous SBA-15 for Efficient Pharmaceutical Removal from Wastewater

Hajar Tallouzt,[a,b] Céline Nayral,[c] Jamal El Haskouri,[d] Khalil Anis,[a] Abdelhak Kherbeche,[a] Abdelkrim El Kadib,[b,e]*

[a] Laboratory of Materials, Process, Catalysis and Environment, Higher School of Technology, Sidi Mohamed Ben Abdellah University, Fez, Morocco

[b] Euro-Med University of Fes (UEMF), Fès, Morocco

[c] Laboratoire de Physique et Chimie des Nano-Objets, Université de Toulouse, CNRS, INSA, UPS, Toulouse CEDEX-4 31077, France

[d] Instituto de Ciència de los Materials de la Universidad de Valencia, Calle catedratico Jose´ Beltran, 2 CP 46980, Paterna, Valencia, Spain

[e] Hassan II Academy of Science and Technology, Rabat, Morocco.

Figure S1. DRIFT spectra of native SBA-15 Before and after extraction.

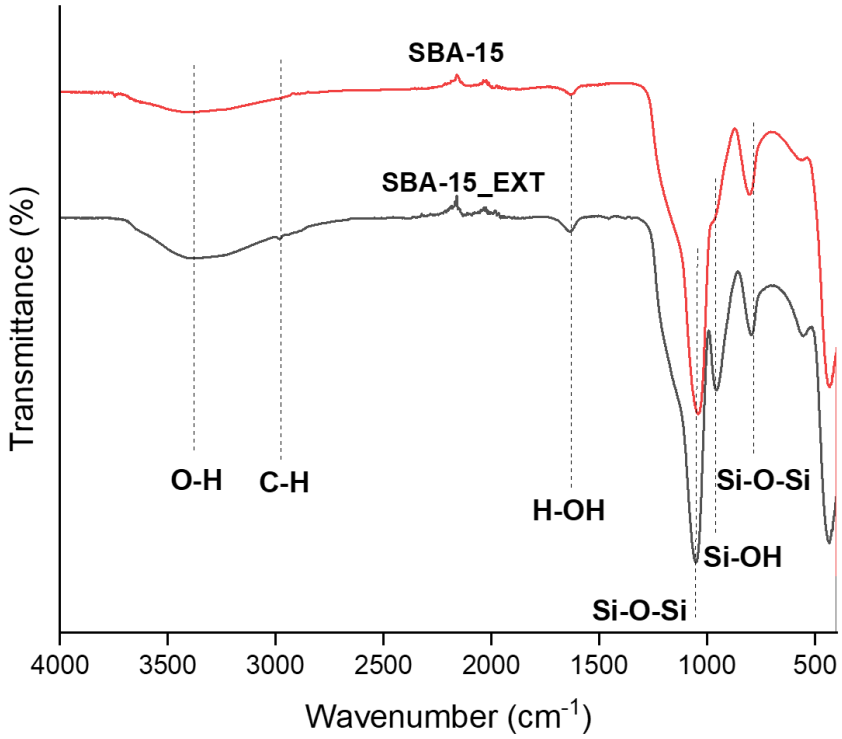

Figure S2. DRIFT spectra of metal oxide on mesoporous silica before and after calcination

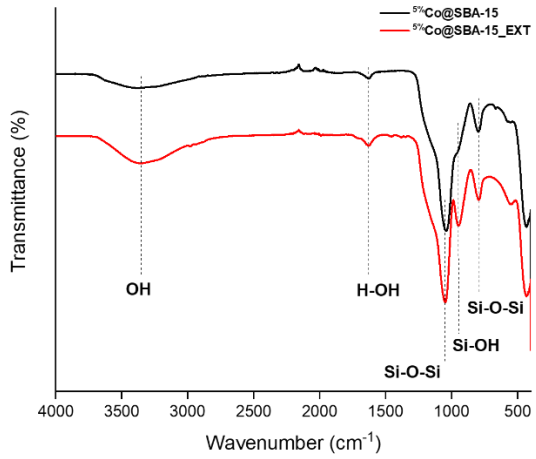

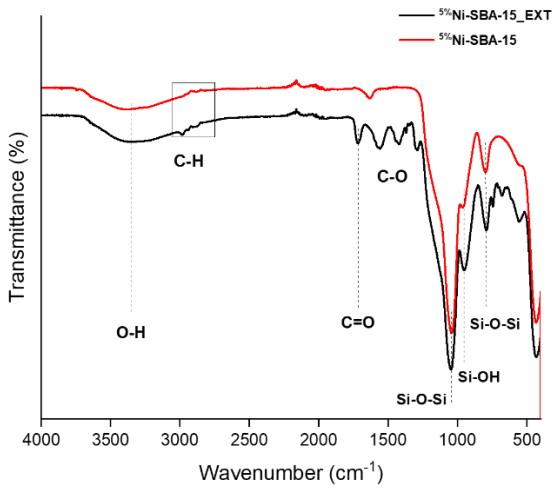

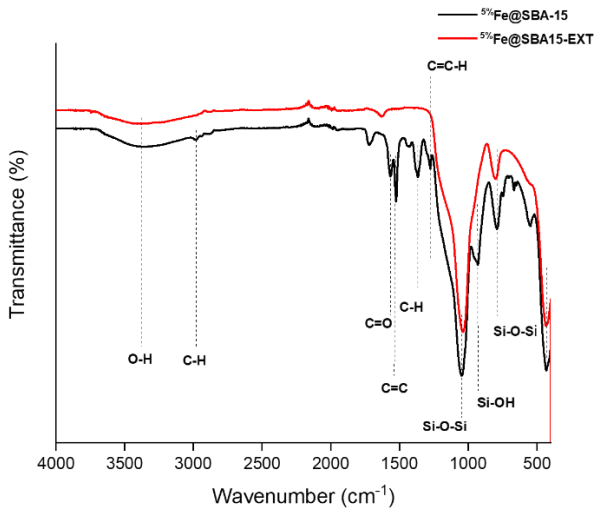

Figure S3. DRIFT spectra of metal-loaded SBA-15

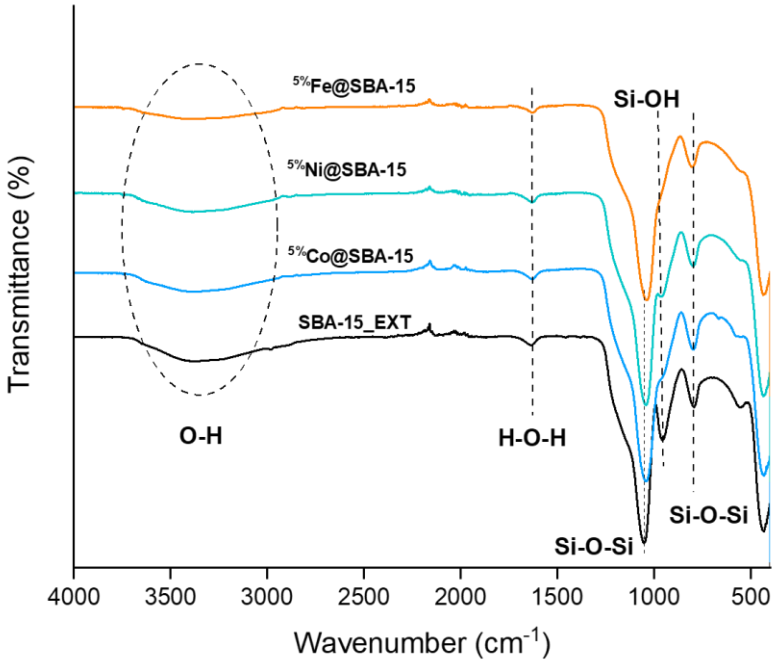

Figure S4. a) and b) ^{29}Si MAS NMR and CP MAS spectra of the calcined **SBA-15_EXT**

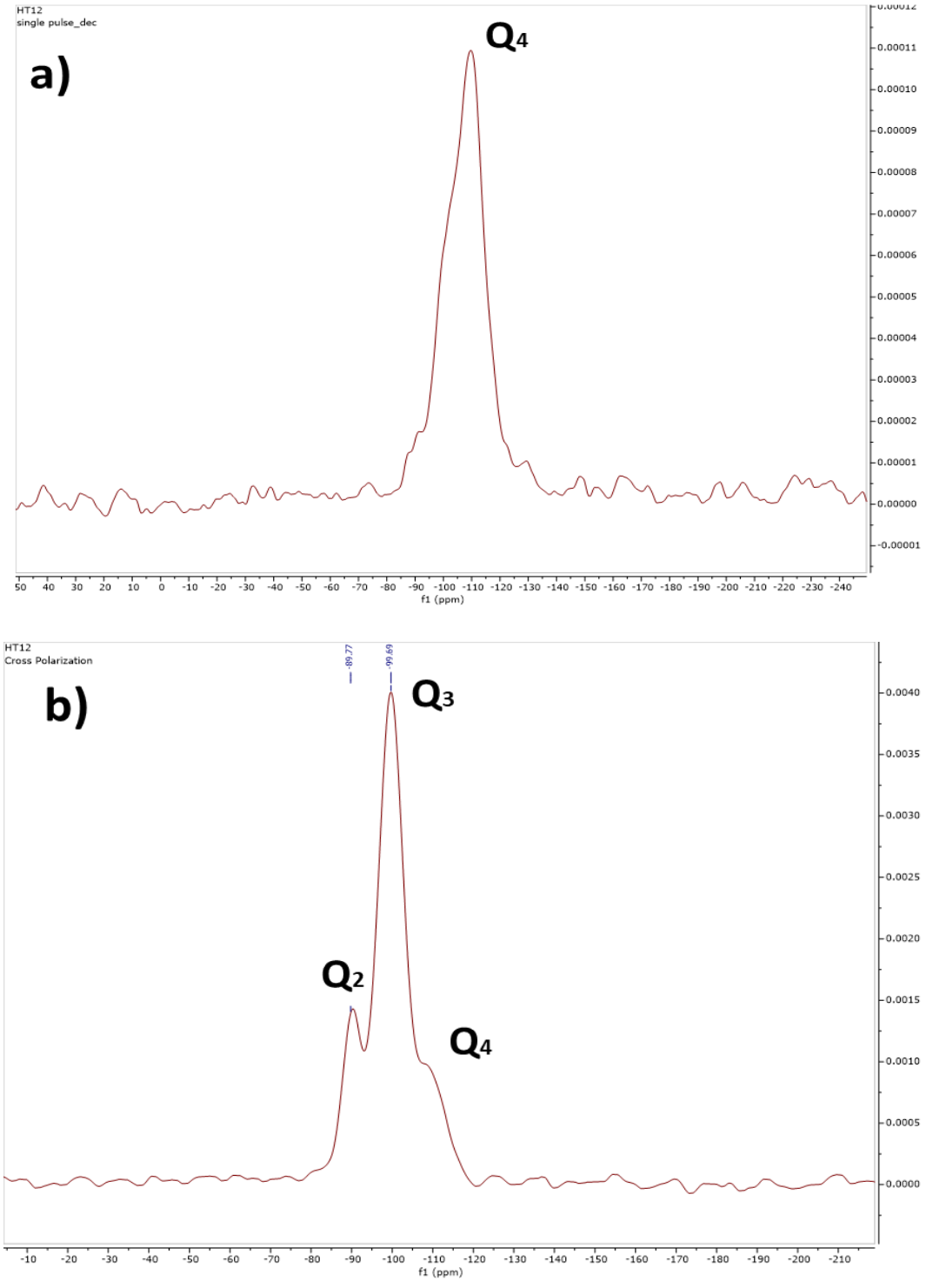

Figure S5. C1) ^{13}C MAS NMR of **SBA-15_EXT** and C2) ^{13}C MAS NMR of **SBA-15**

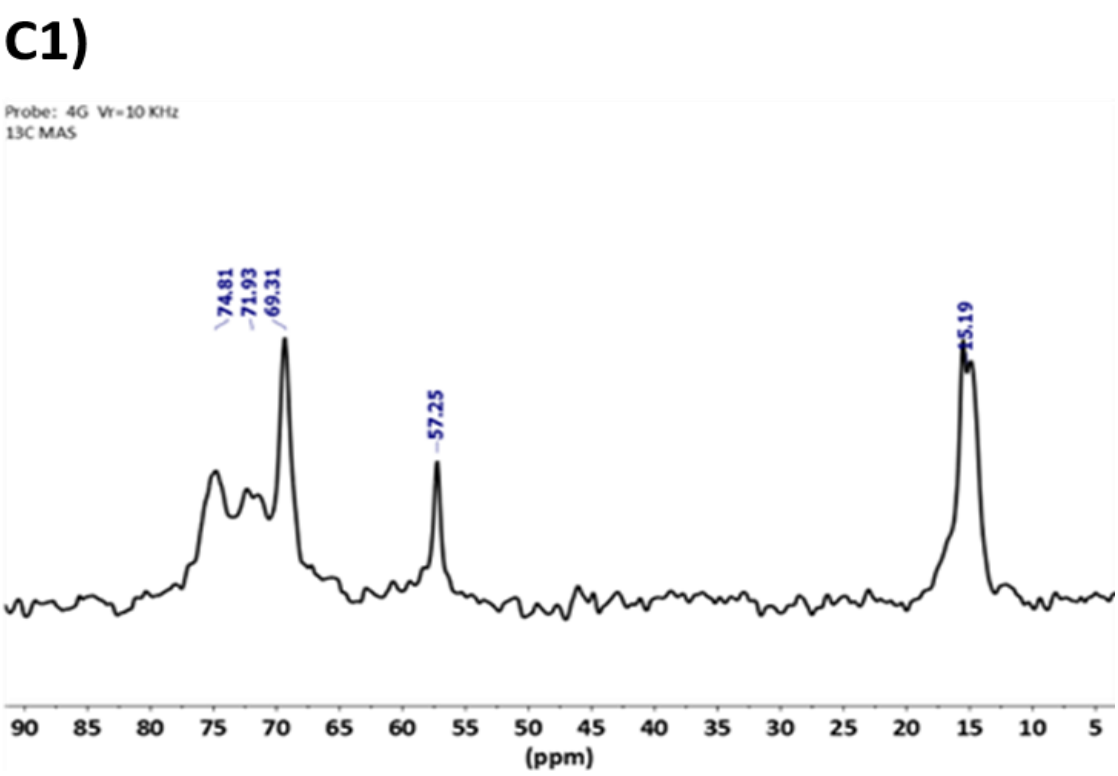

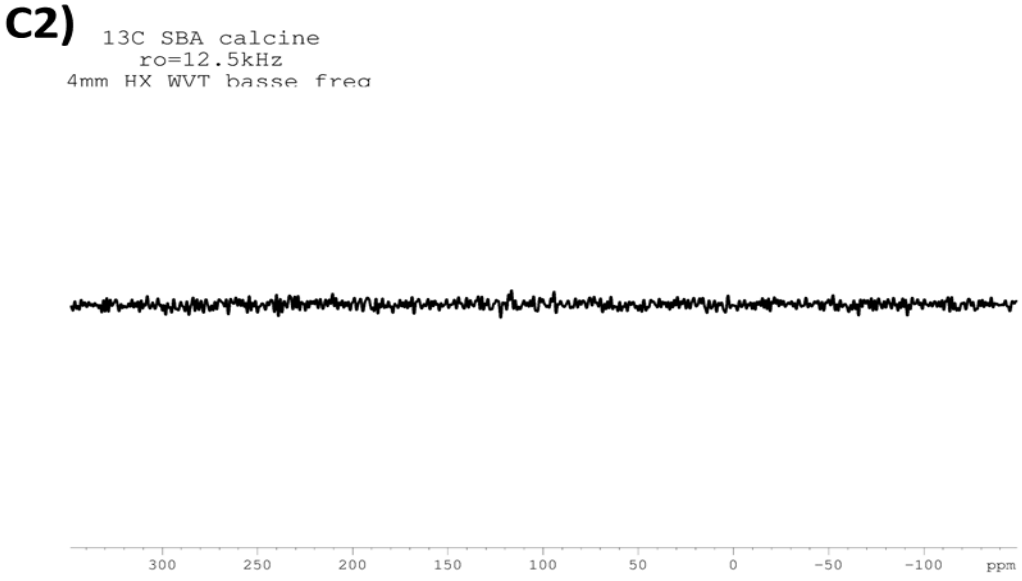

Figure S6. TGA spectra of the materials before and after calcination

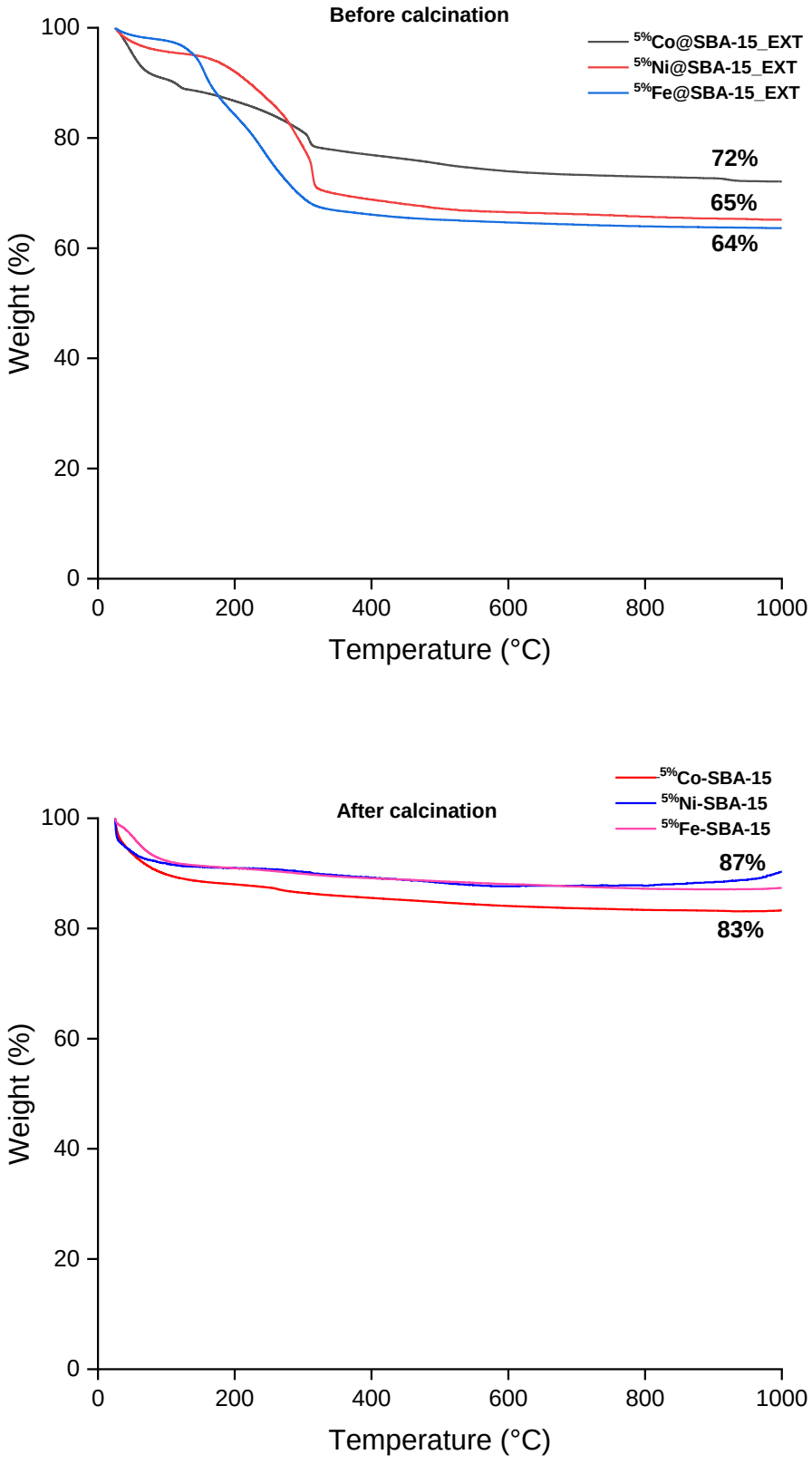

Figure S7. Photos of the suspension

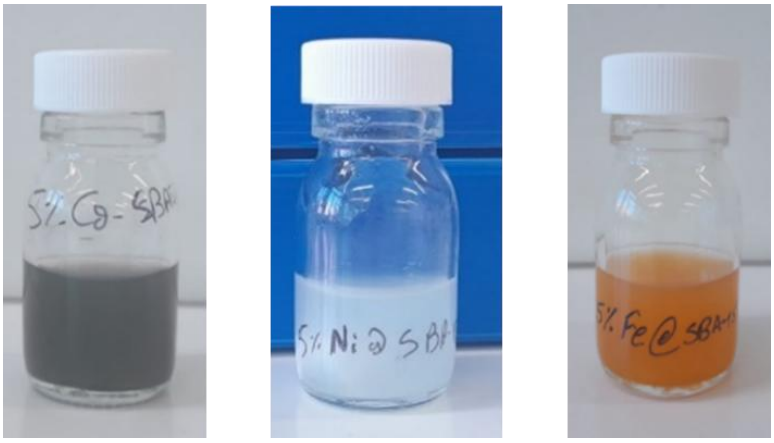

Figure S8. N2 adsorption-desorption of **$^{5\%}$Co@SBA-15-CAL**

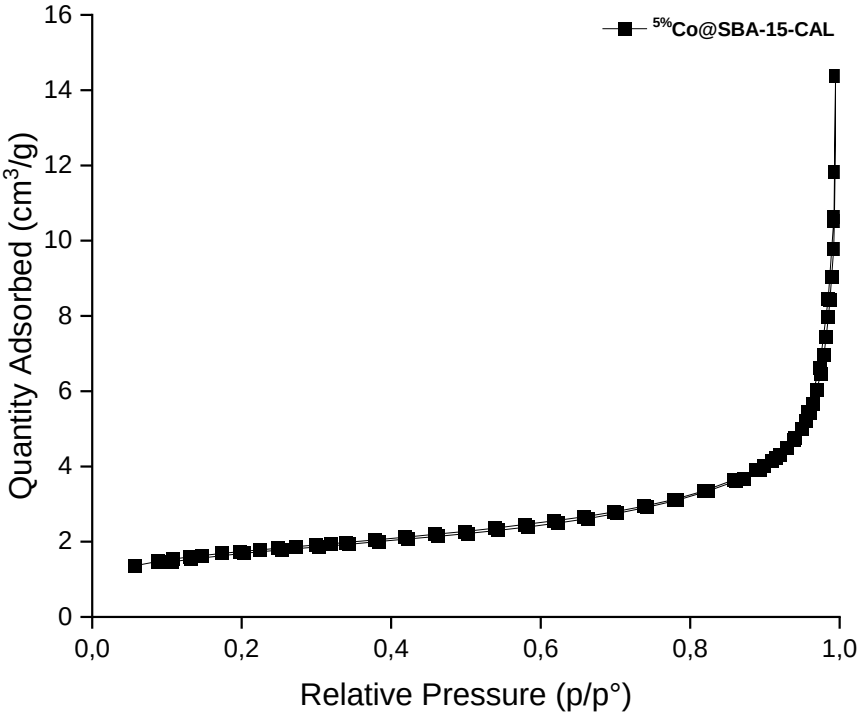

Figure S9. Wide-angle XRD of **$^{5\%}$Co@SBA-15**, **$^{5\%}$Ni@SBA-15** and **$^{5\%}$Fe@SBA-15** versus pristine **SBA-15_EXT**

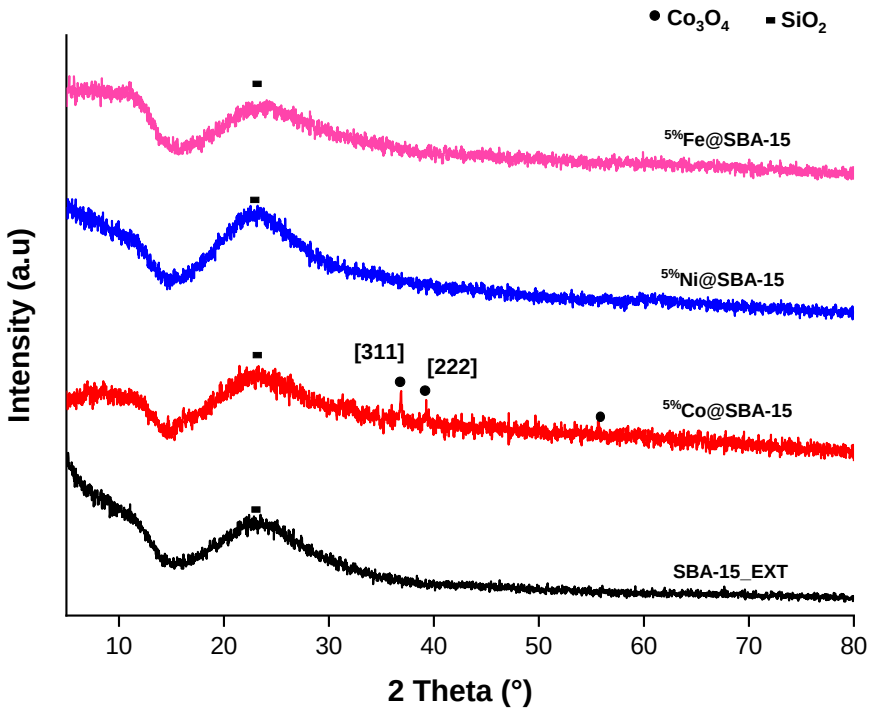

Figure S10. XPS spectra of **$^{5\%}$Co@SBA-15**

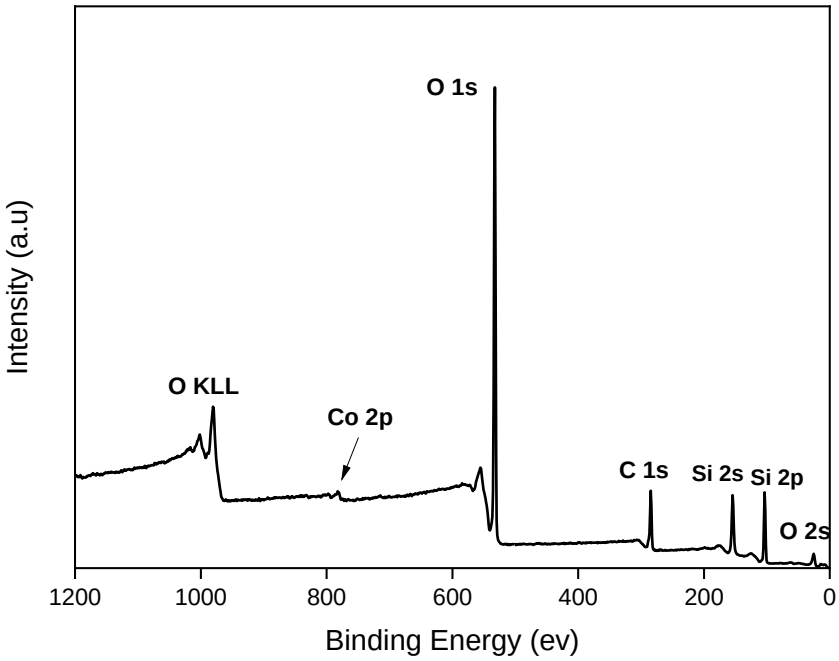

Figure S11. RAMAN

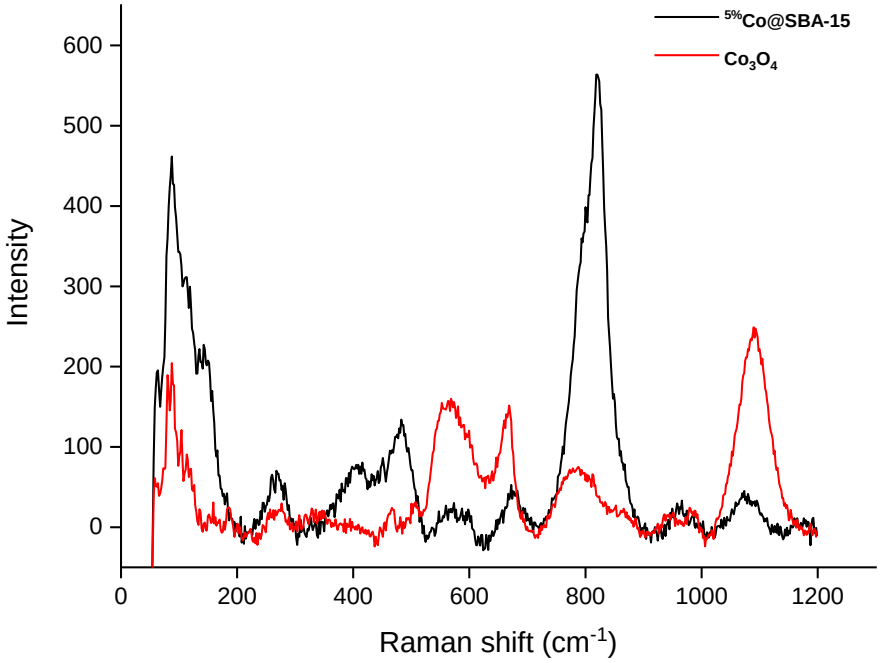

Figure S12. UV-visible spectra of **SBA-15_EXT** and **$^{x\%}$M@SBA-15**

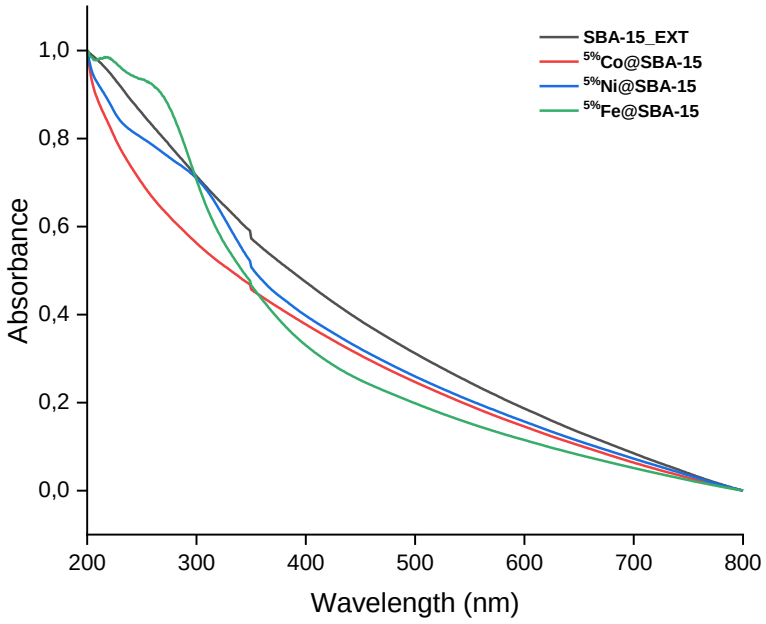

Figure S13. Tauc plot

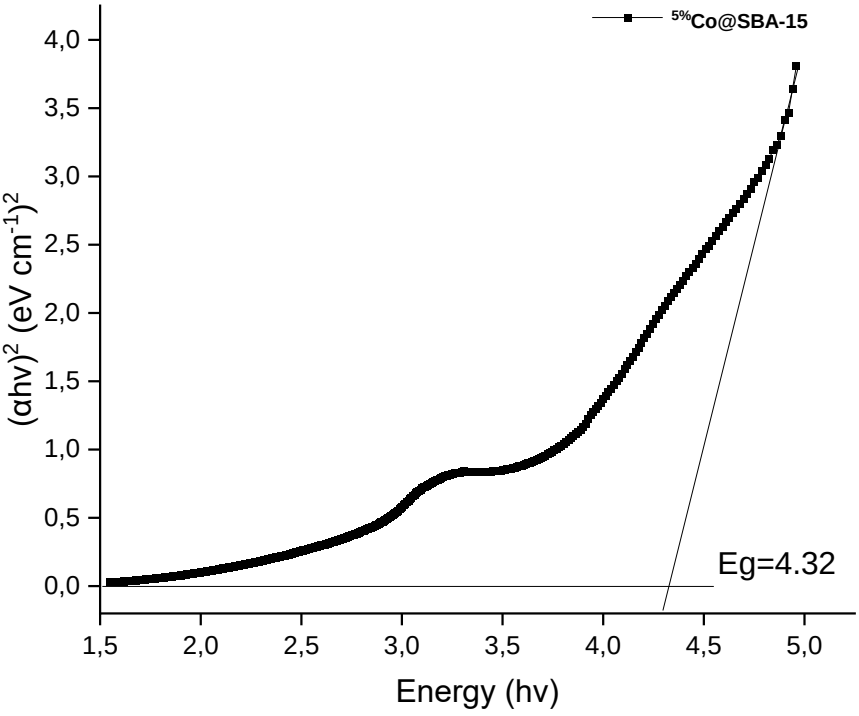

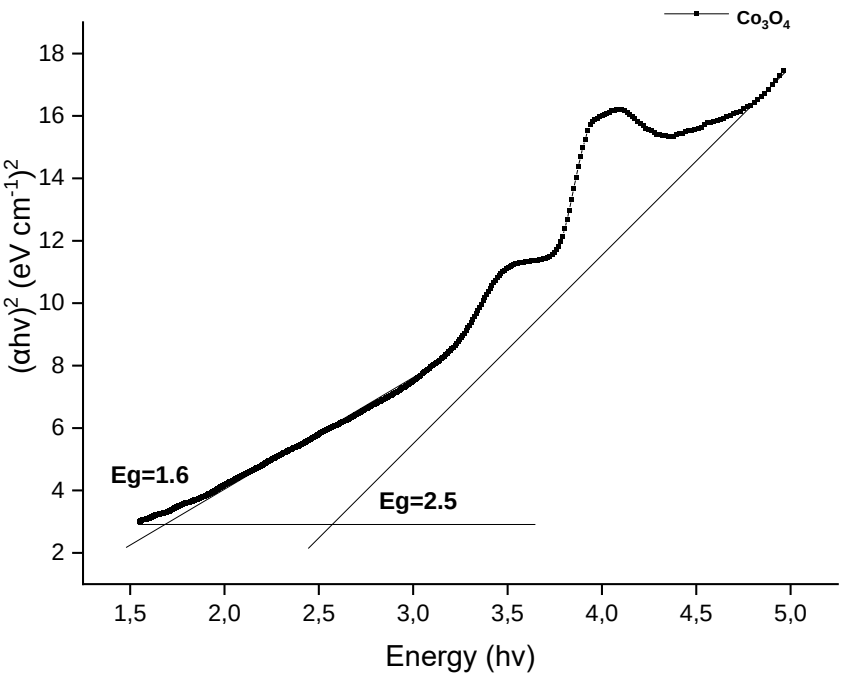

Figure S14. N_2 adsorption-desorption isotherms of **$^{2.5\%}$Co@SBA-15**, **$^{5\%}$Co@SBA-15**, **$^{7.5\%}$Co@SBA-15** and **SBA-15_EXT.**

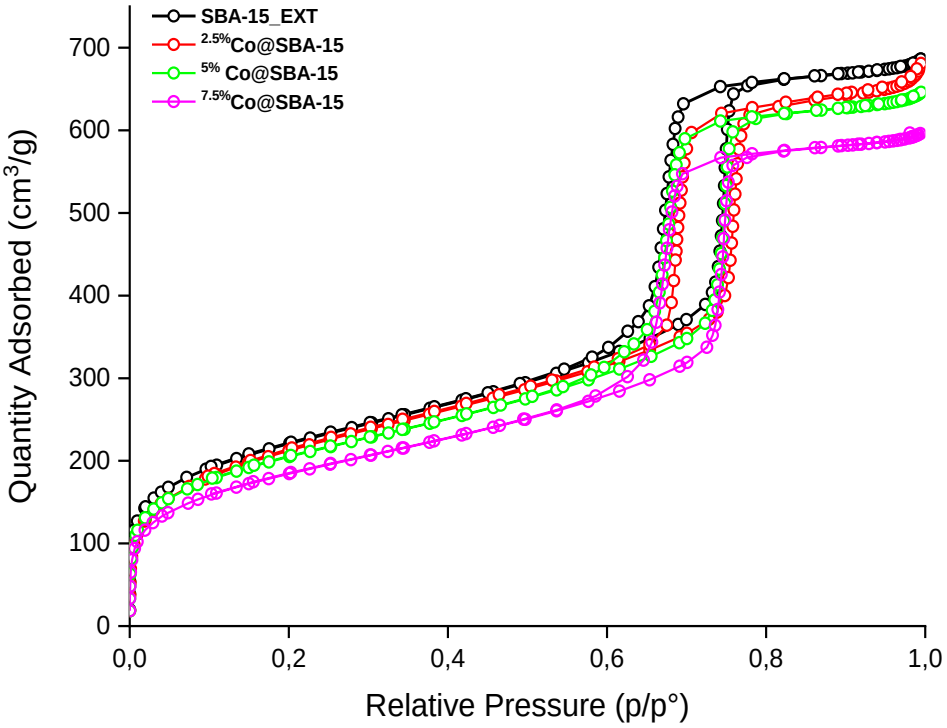

Figure S15. DRIFT spectra of **$^{5\%}$Co@SBA-15** before and after trimethylsilylation

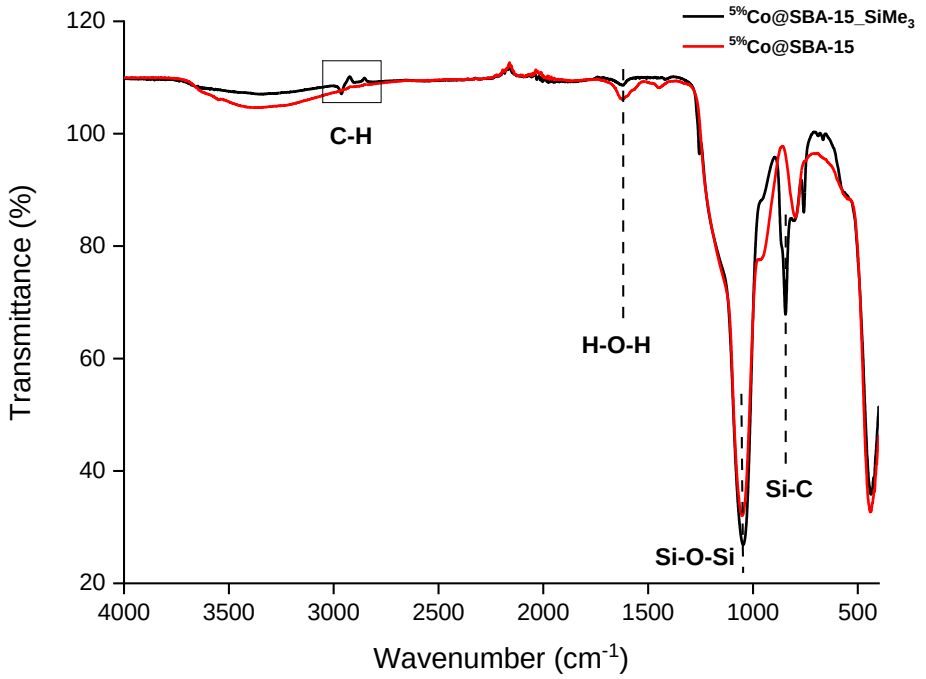

Figure S16. Solid state MAS ^{13}C NMR of **$^{5\%}$Co-SBA-15-SiMe$_3$**

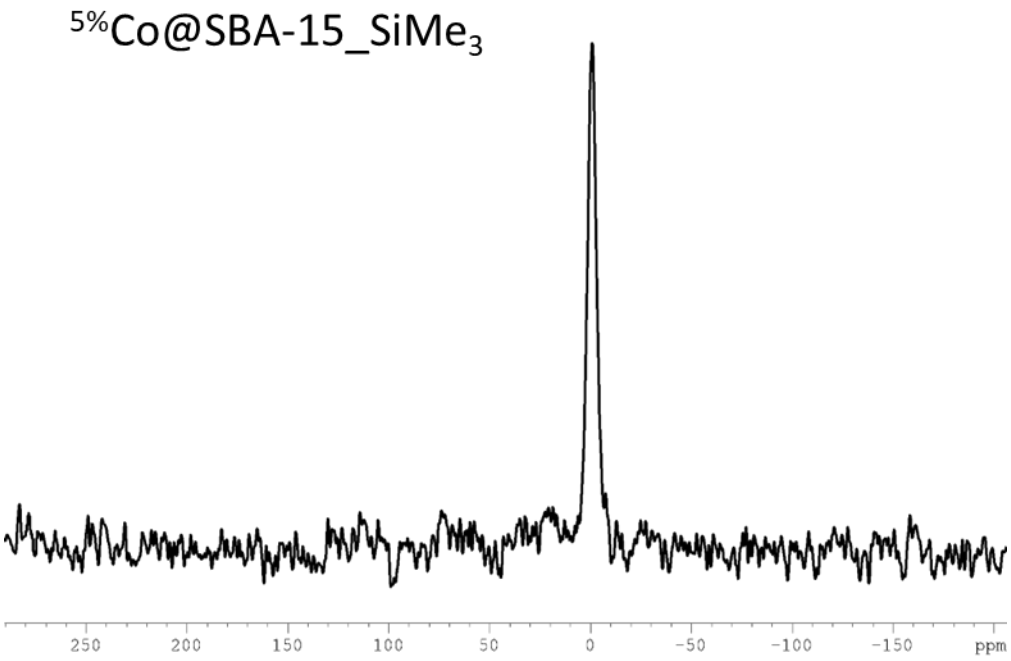

Figure S17. DRIFT spectra of (a) **SBA-NH$_2$_EXT**, (b) **SBA-NNH$_2$_EXT**, (c) **SBA-NNNH$_2$_EXT** and (d) **SBA-SH_EXT** before and after soxhlet extraction

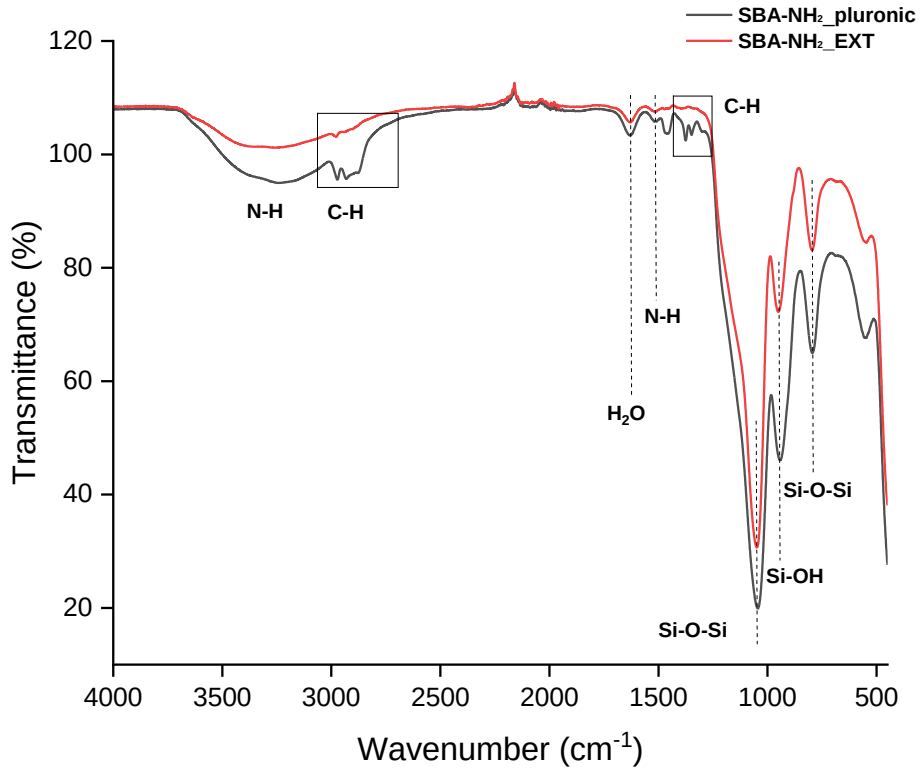

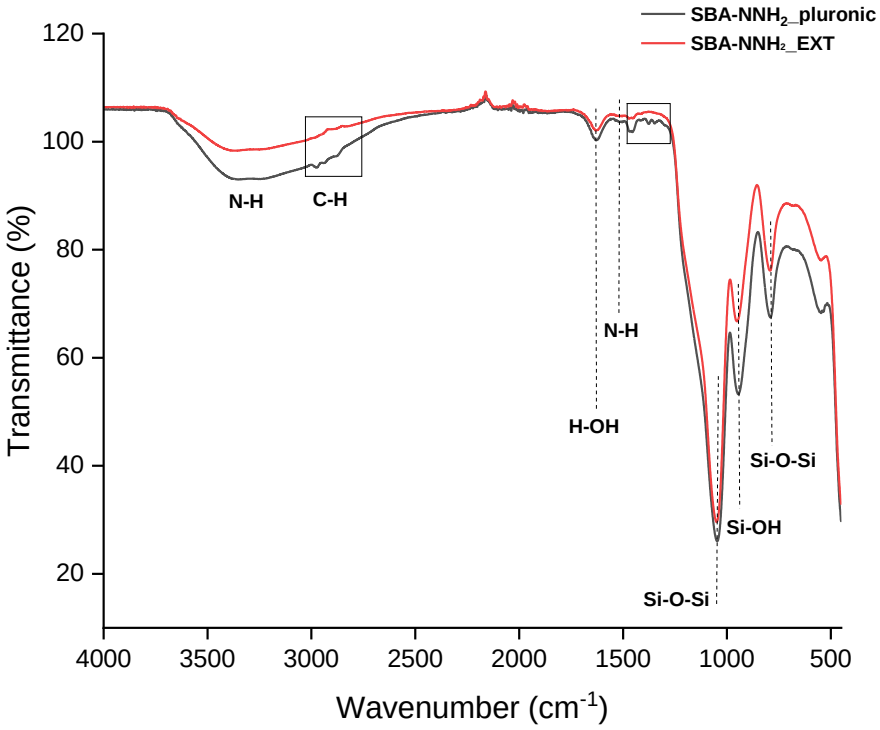

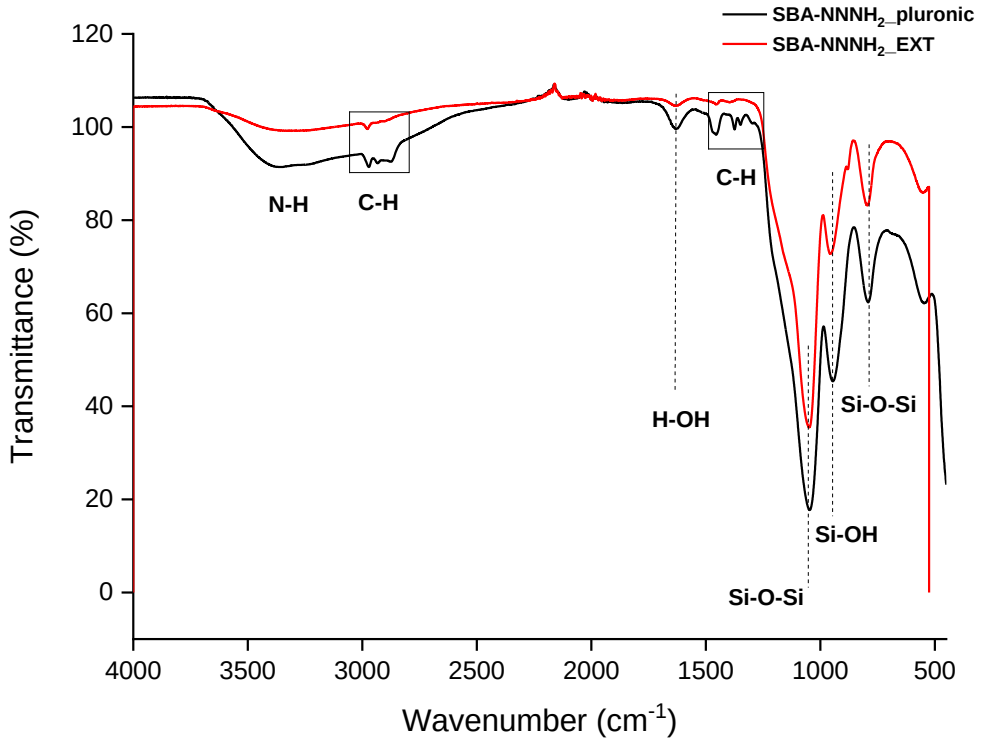
SBA-NNNH2_pluronic
SBA-NNNH2_EXT
Transmittance (%)
Wavenumber (cm-1)
N-H
C-H
C-H
H-OH
Si-O-Si
Si-OH
Si-O-Si

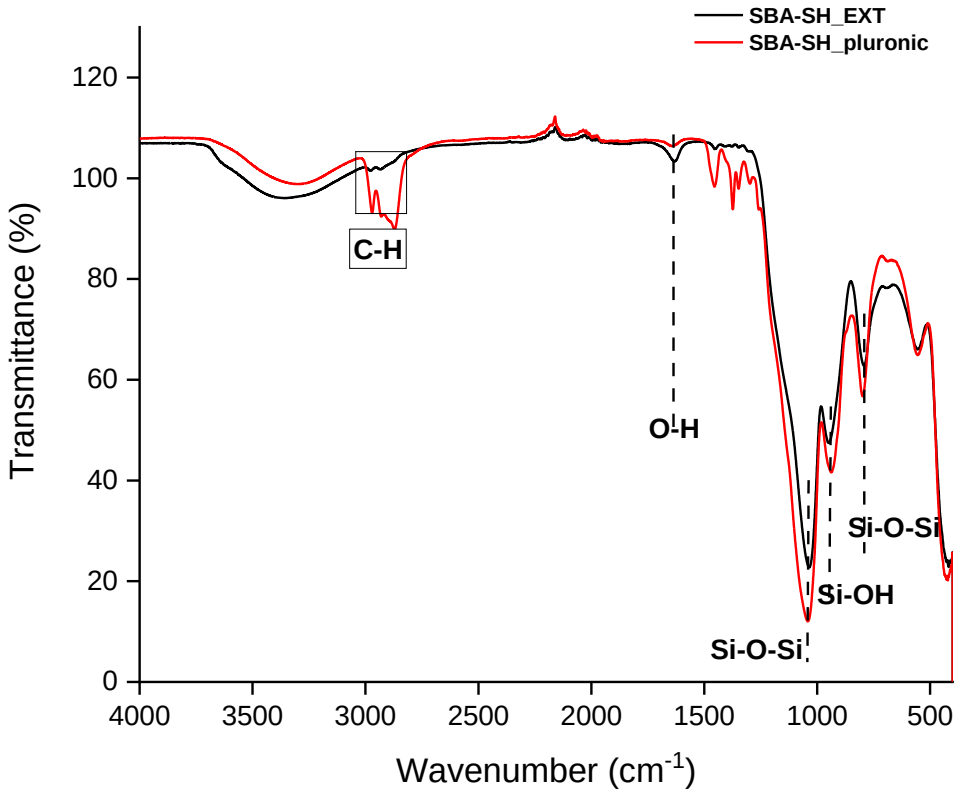
SBA-SH_EXT
SBA-SH_pluronic
Transmittance (%)
Wavenumber (cm-1)
C-H
O-H
Si-O-Si
Si-OH
Si-O-Si

Figure S1*8*. SEM images of **SBA-OH_EXT**, **SBA-NH$_2$_EXT**, **SBA-NNH$_2$_EXT**, **SBA-NNNH$_2$_EXT** and **SBA-SH_EXT**

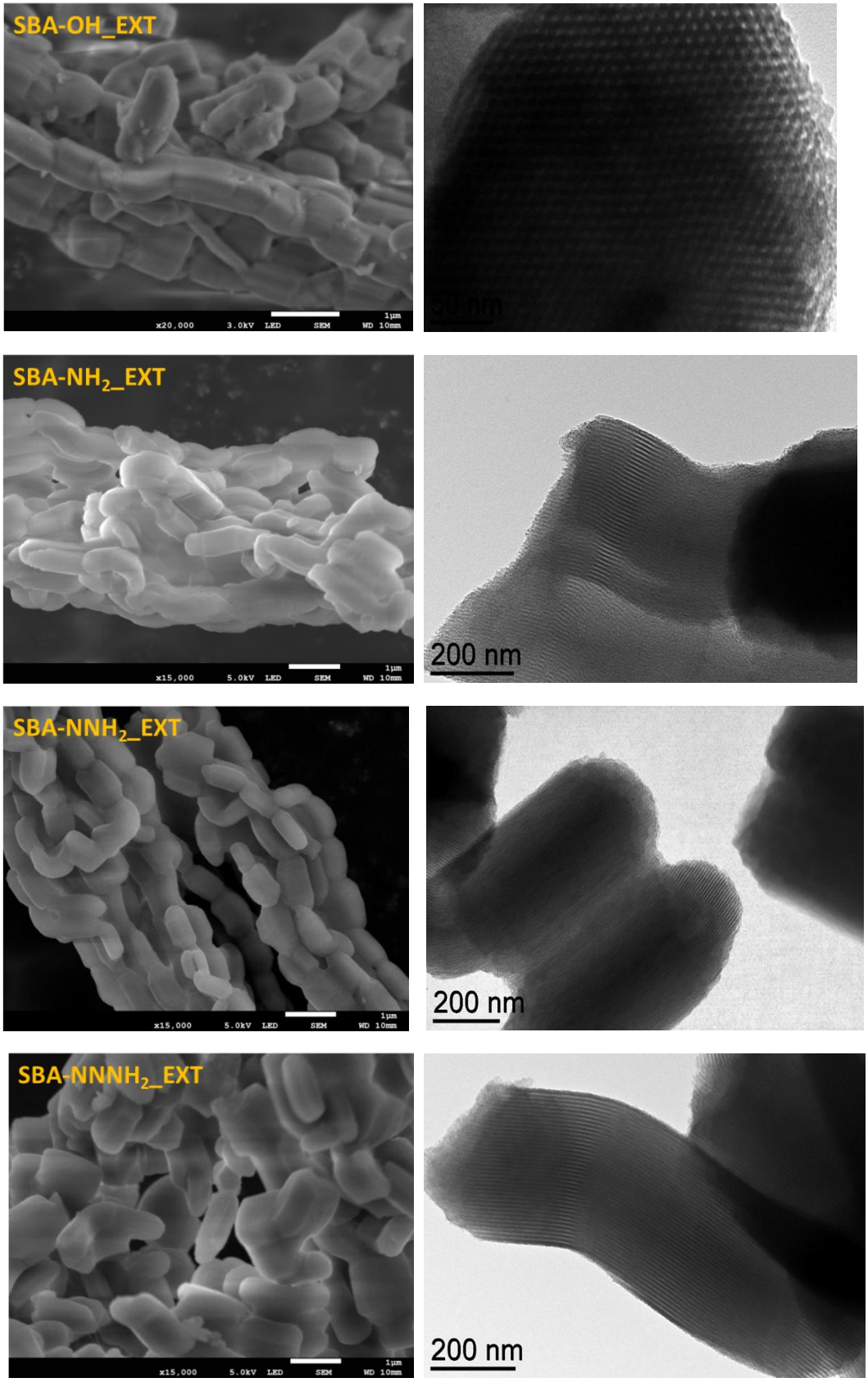

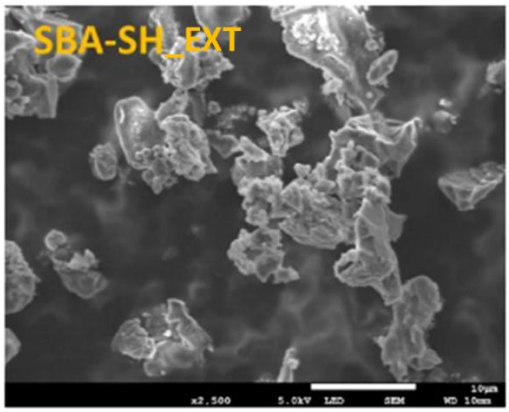
SBA-SH_EXT
x2,500 5.0kV LED SEM WD 10mm
10µm

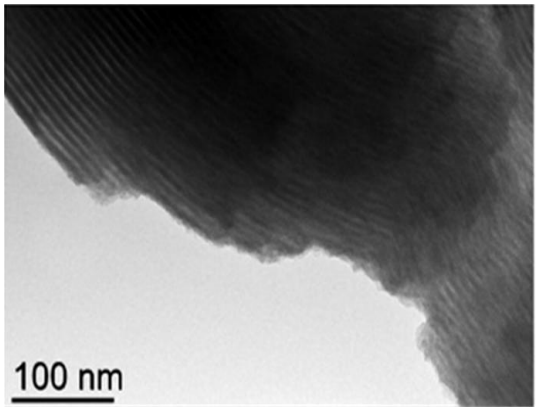
100 nm

Figure S19. N_2 adsorption-desorption isotherms of **SBA-NH_2_EXT**, **SBA-NNH_2_EXT**, **SBA-$NNNH_2$_EXT** and **SBA-SH_EXT**

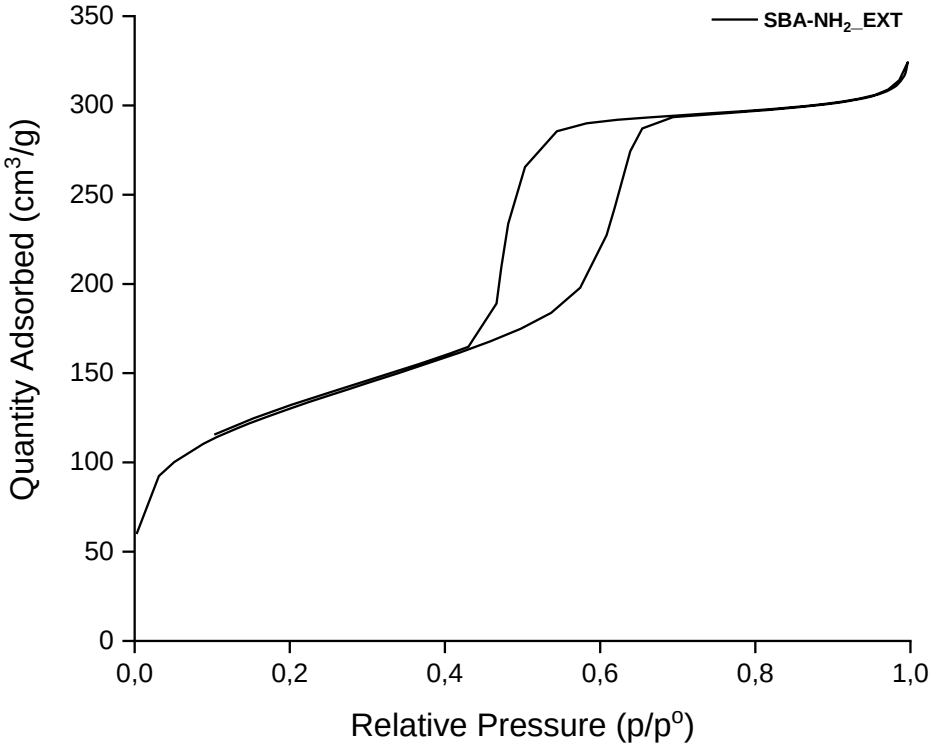

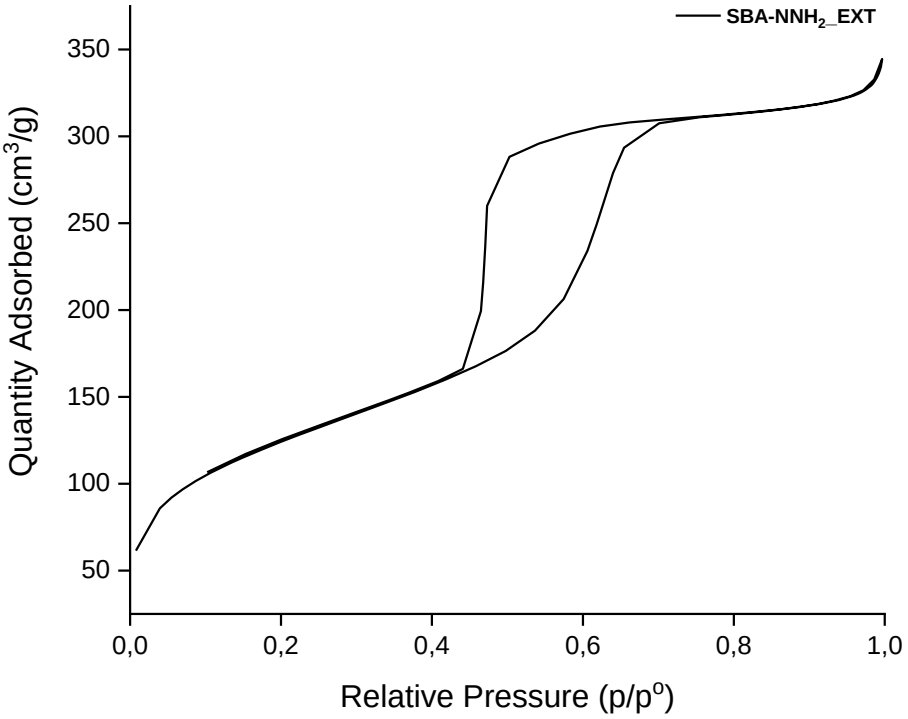

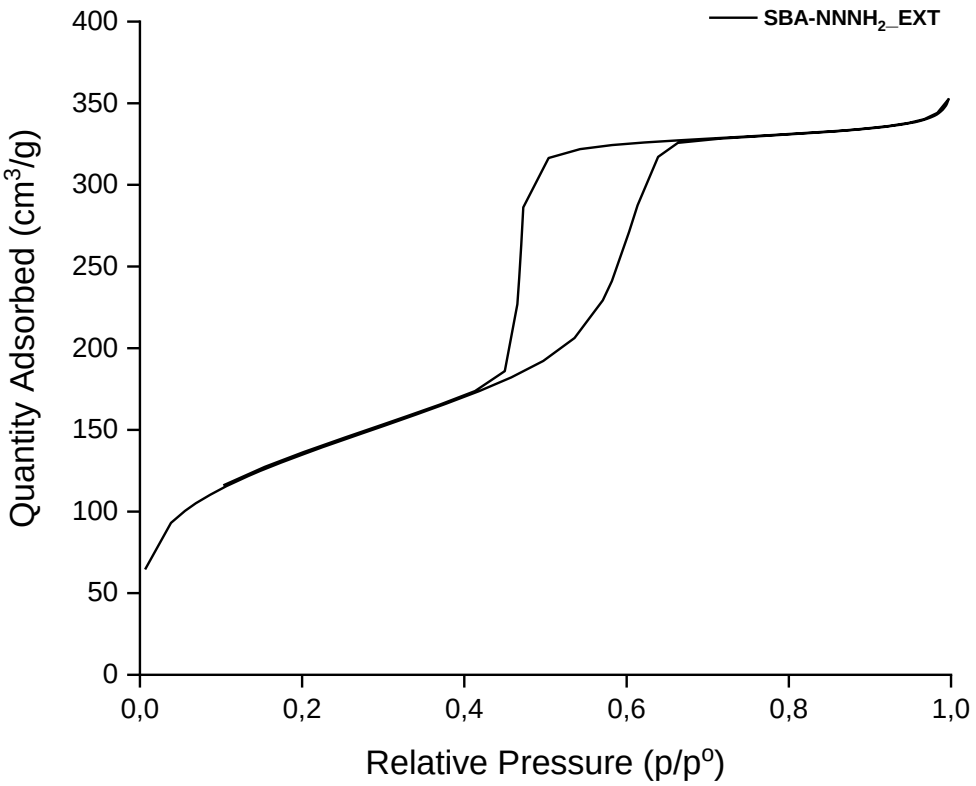
SBA-NNNH2_EXT
Quantity Adsorbed (cm3/g)
Relative Pressure (p/po)
0
50
100
150
200
250
300
350
400
0,0
0,2
0,4
0,6
0,8
1,0

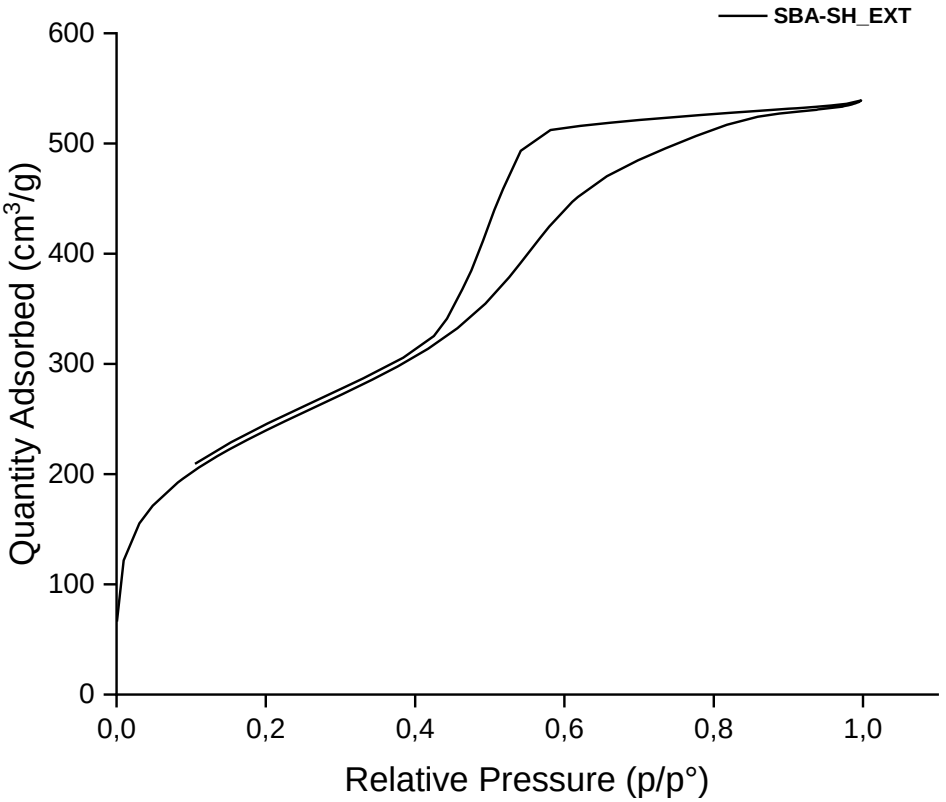
SBA-SH_EXT
Quantity Adsorbed (cm3/g)
Relative Pressure (p/p°)
0
100
200
300
400
500
600
0,0
0,2
0,4
0,6
0,8
1,0

Figure S20. Zeta potential of $^{7.5\%}$**Co@SBA-15**

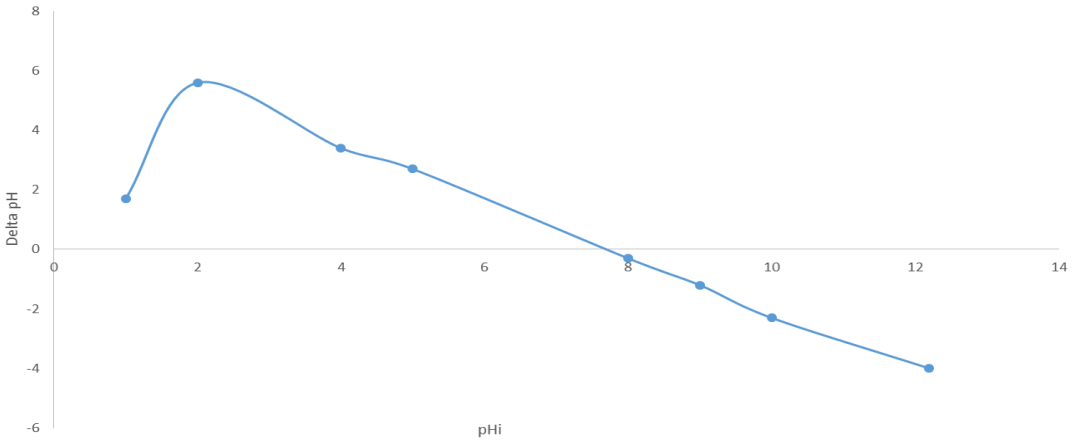

Figure S21. DRIFT of $^{5\%}$**Co@SBA-15** before and after adsorption

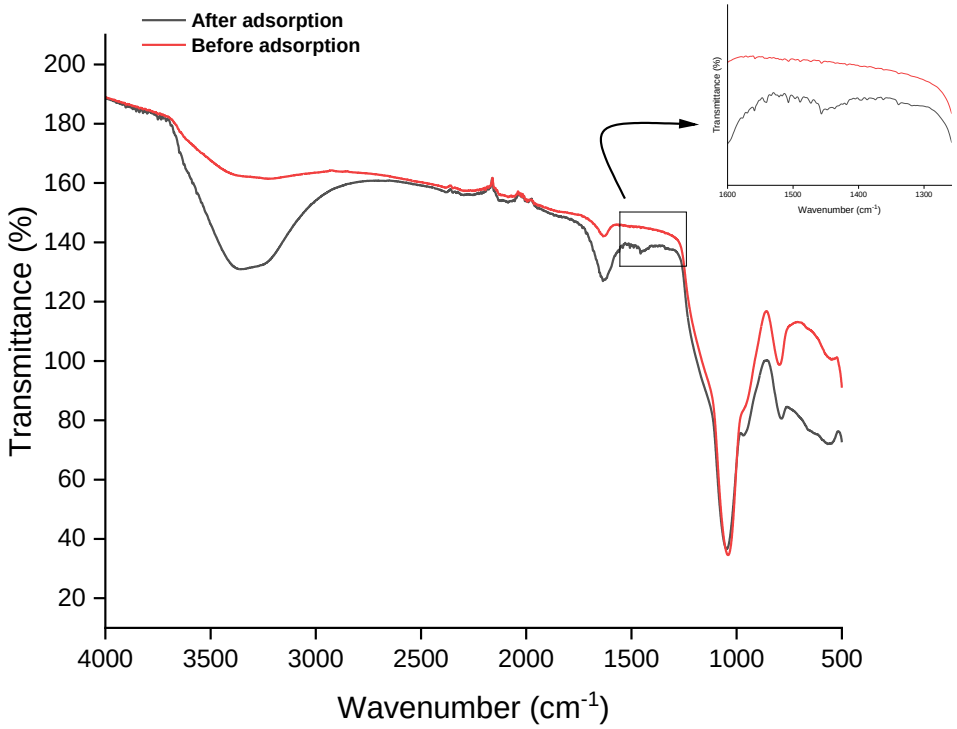

Figure S22. Adsorption of concentrated tetracycline solution (10^{-3} mol.L^{-1})

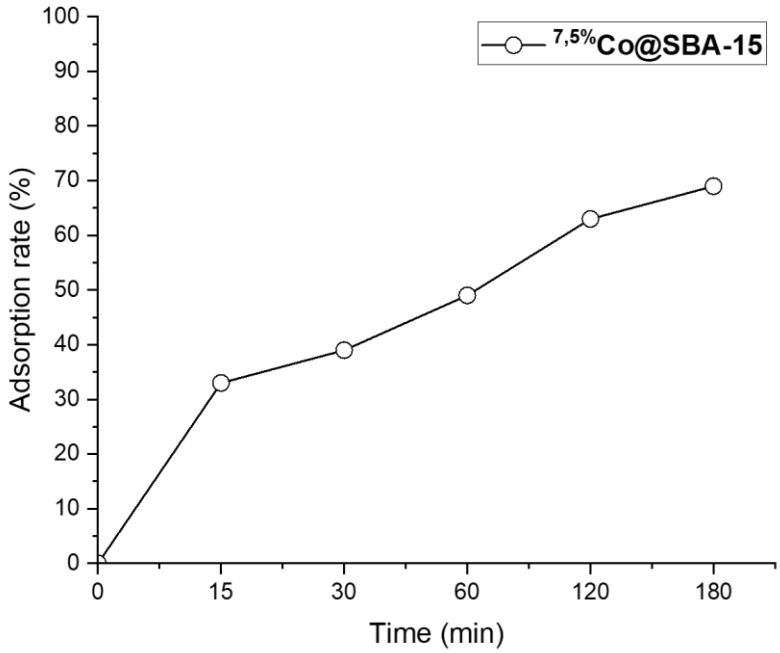

Figure S23. Adsorption versus photo-catalysis of concentrated tetracycline solution

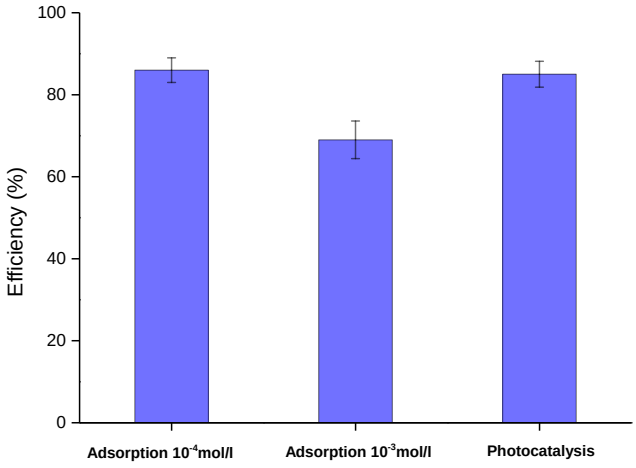

Figure S24. Total organic content

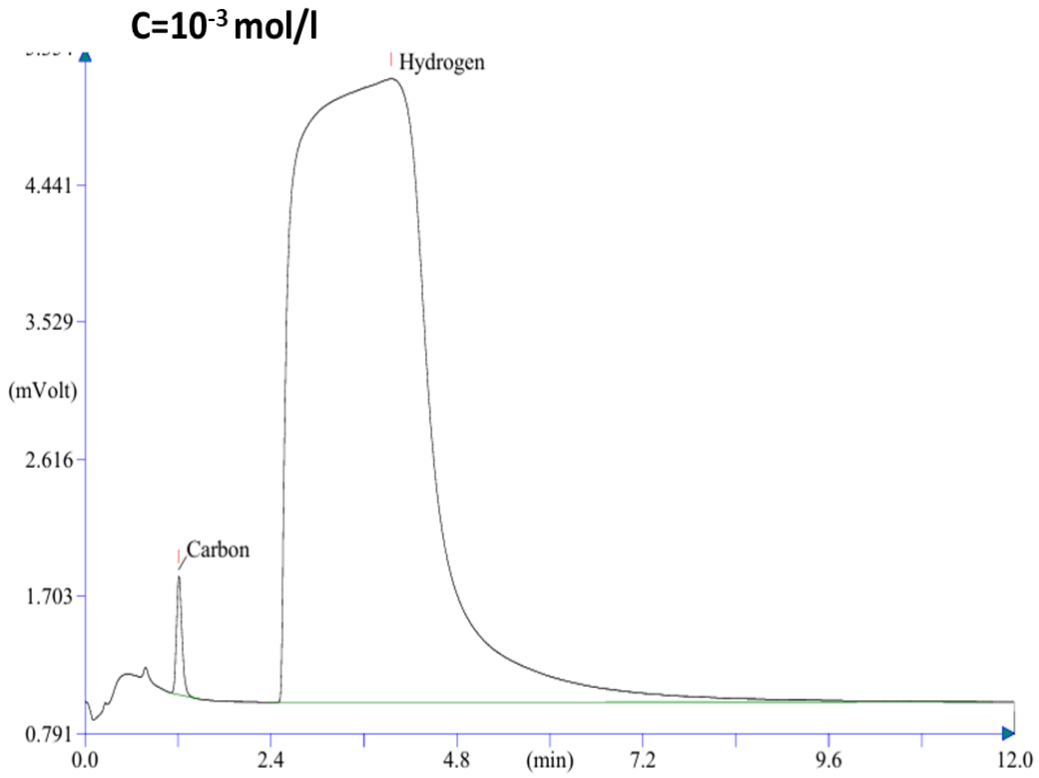

Element Name	%	Ret.Time	Area	BC	Area ratio
Carbon	0.5939	73	38706	RS	1.000000
Hydrogen	11.7299	237	4912214	RS	.007879

After 3 hours of adsorption

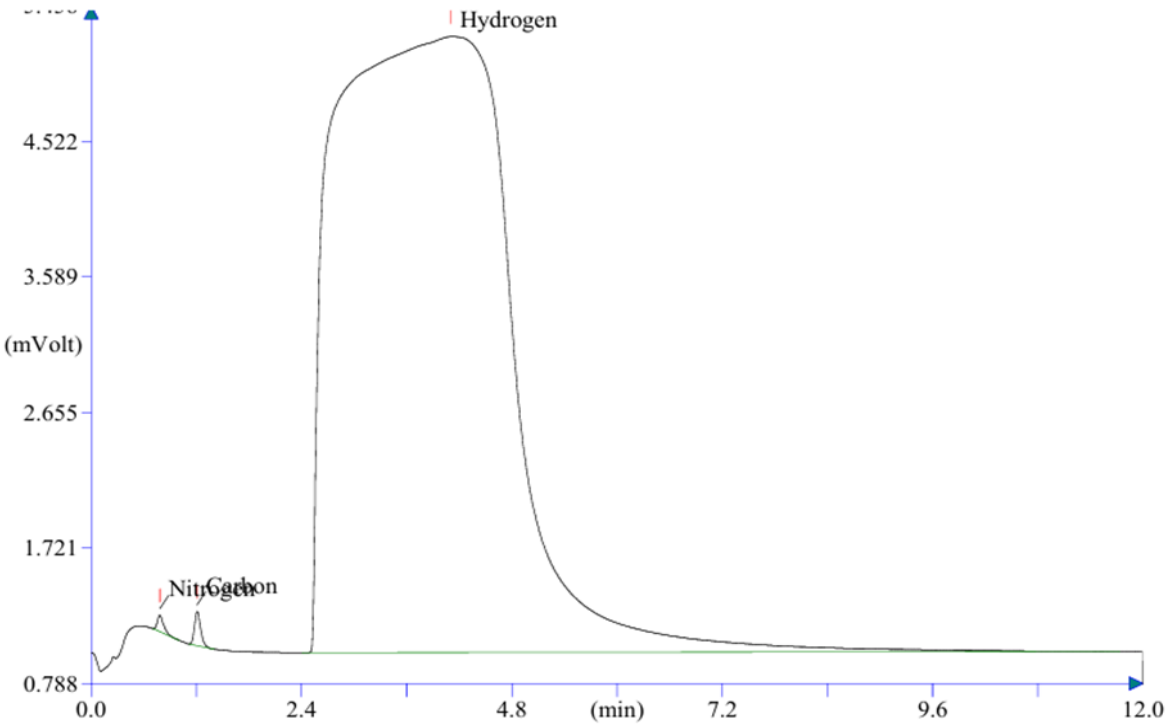

Element Name	%	Ret.Time	Area	BC	Area ratio
Nitrogen	0.3294	47	5282	RS	2.173436
Carbon	0.3874	73	11479	RS	1.000000
Hydrogen	14.0115	247	5887544	RS	.001950

After 3 hours of irradiation

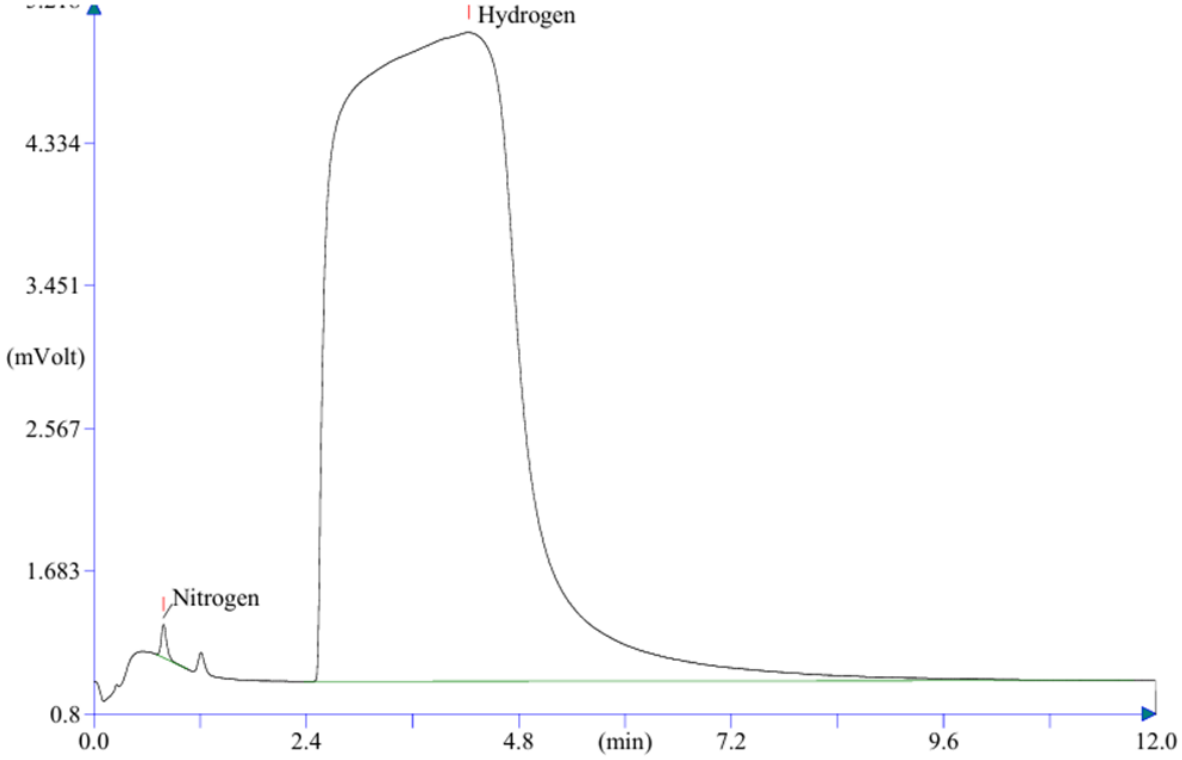

Element Name	%	Ret.Time	Area	BC	Area ratio
Nitrogen	0.3909	47	8566	RS	.000000
Hydrogen	13.2943	254	5580931	RS	.000000

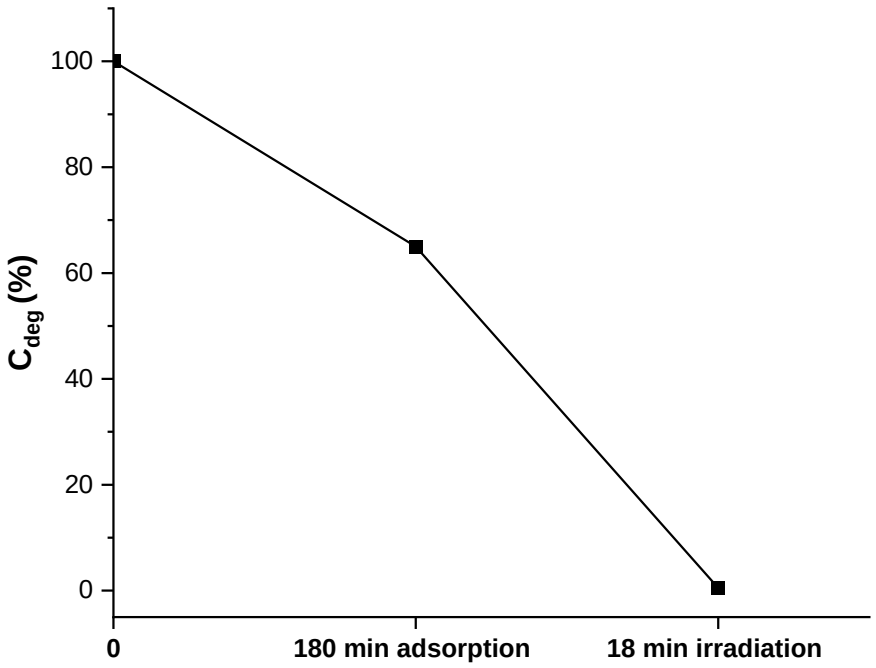

Steps	TOC %	C_{deg} (%)
Initial (t=0 h)	0.59	0
After 3h of adsoption	0.39	35
After 3h of irradiation	≈0	≈ 100

Table S1. TGA curve of metal-loaded mesoporous materials before and after thermal treatment

Samples	T_{10}	% char residue
$^{5\%}$Co@SBA-15	94	83
$^{5\%}$Ni@SBA-15	315	87
$^{5\%}$Fe@SBA-15	285	87
$^{5\%}$Co@SBA-15_EXT	112	72
$^{5\%}$Ni@SBA-15_EXT	220	65
$^{5\%}$Fe@SBA-15_EXT	163	64

Table S2. Textural characterization of **$^{2.5\%}$Co@SBA-15**, **$^{5\%}$Co@SBA-15** and **$^{7.5\%}$Co@SBA-15**

Samples	Nitrogen sorption isotherms		
	S_{BET} ($m^2.g^{-1}$)	V_{mesop} (ml/g)	Pore diameter (A°)
$^{2.5\%}$Co@SBA-15	753	0.95	62
$^{5\%}$Co@SBA-15	722	0.93	69
$^{7.5\%}$Co@SBA-15	654	0.87	61

Table S3. Textural characterization of modified **SBA-15**

Samples	Nitrogen sorption isotherms		
	S_{BET} ($m^2.g^{-1}$)	V_{mesop} (ml/g)	Pore diameter (A°)
SBA-NH_2_EXT	448	0.5	52
SBA-NNH_2_EXT	441	0.53	52
SBA-$NNNH_2$_EXT	478	0.54	49
SBA-SH_EXT	618	0.66	67

Table S4. Comparison of the adsorption performance of tetracycline: materials reported in the literature vs. our material

Materials	[TC] (mg/l	pH	Equilibrium Time	Qm (mg/g)	References
Cu/SBA-15	50	7	1200 min	961.54	[1]
SBA-15@NU-1000	40	3-10	10 min	424	[2]
Fe_{30}SBA-15	100	7	36 h	41.7	[3]
Fe-SBA15	48,09	5	24h	74.95	[4]
PGOSBA	100	7	16h	29.2	[5]
$^{5\%}$Co@SBA-15	48.09 480.9	7 7	180 min 180 min	41.31 331.821	This work

Table S5. Table of photocatalytic efficiency in tetracycline degradation: literature vs. our results

Materials	**[TC] (mg/l)**	**pH**	**Time**	**% reduction**	**References**
(SBA-15)/CeO_2	192.36	7	90 min	90.18 %	[6]
g-C_3N_4(3.0) /W-SBA-15	48.09	-	160 min	98.2 %	[7]
B-g-C_3N_4/SBA-15	20	-	120 min	93.74 %	[8]
mpg-C3N4	20	-	60 min	86%	[9]
Gr5- SBA/TiO2	50	-	30 min	89 %	[10]
$^{5\%}$Co@SBA-15	480.9	-	420 min	85 %	This work

References:

(1) Qiu, Y.; Kong, L.; Chen, T.; Xu, Q. Efficient Adsorption of Tetracycline Using Cu+-Modified SBA-15 and Its Adsorption Mechanism. *Journal of Environmental Engineering* **2020**, *147* (1), 04020142. https://doi.org/10.1061/(ASCE)EE.1943-7870.0001813.

(2) Yang, J.; Wu, J.; Gao, L.; Duan, L. H.; Wang, J. Amino Functional SBA-15 Assisted NU-1000 for the Rapid and Efficient Adsorption of Tetracycline Antibiotics. *New Journal of Chemistry* **2024**, 19101–19112. https://doi.org/10.1039/d4nj03736g.

(3) Vu, B. K.; Shin, E. W.; Snisarenko, O.; Jeong, W. S.; Lee, H. S. Removal of the Antibiotic Tetracycline by Fe-Impregnated SBA-15. *Korean Journal of Chemical Engineering* **2010**, *27* (1), 116–120. https://doi.org/10.1007/S11814-009-0313-5/METRICS.

(4) Zhang, Z.; Lan, H.; Liu, H.; Li, H.; Qu, J. Iron-Incorporated Mesoporous Silica for Enhanced Adsorption of Tetracycline in Aqueous Solution. *RSC Adv* **2015**, *5* (53), 42407–42413. https://doi.org/10.1039/C5RA05478H.

(5) Xikhongelo, R. V.; Mtunzi, F. M.; Diagboya, P. N.; Olu-Owolabi, B. I.; Düring, R. A. Polyamidoamine-Functionalized Graphene Oxide-SBA-15 Mesoporous Composite: Adsorbent for Aqueous Arsenite, Cadmium, Ciprofloxacin, Ivermectin, and Tetracycline. *Ind Eng Chem Res* **2021**, *60* (10), 3957–3968. https://doi.org/10.1021/ACS.IECR.0C04902/ASSET/IMAGES/LARGE/IE0C04902_0005.JPEG.

(6) Boonyuen, S.; Smith, S. M.; Luengnaruemitchai, A.; Nakorn, P. N.; Tangjaideborisu, Y.; Shanmugam, P. Amplified Photocatalytic Decay of Organic Dyes and Antibiotic Pollutants Using Hexagonal Honeycomb Mesoporous Silica (SBA-15)/CeO2 Nanocomposites under Visible-Light Exposure. *Inorg Chem Commun* **2025**, *173*, 113862. https://doi.org/10.1016/J.INOCHE.2024.113862.

(7) Duan, Y.; Cao, Y.; Shang, X.; Jia, D.; Li, C. Synthesis of G-C3N4/W-SBA-15 Composites for Photocatalytic Degradation of Tetracycline Hydrochloride. *J Inorg Organomet Polym Mater* **2021**, *31* (5), 2140–2149. https://doi.org/10.1007/S10904-021-01923-4/FIGURES/9.

(8) Shanmugam, P.; Smith, S. M.; Boonyuen, S.; Luengnaruemitchai, A. In-Situ Development of Boron Doped g-C3N4 Supported SBA-15 Nanocomposites for Photocatalytic Degradation of Tetracycline. *Environ Res* **2023**, *224*, 115496. https://doi.org/10.1016/J.ENVRES.2023.115496.

(9) Liu, H.; Wu, H.; Lv, J.; Xu, G.; Chen, X.; Zhang, X.; Wu, Y. SBA-15 Templated Mesoporous Graphitic C3N4 for Remarkably Enhanced Photocatalytic Degradation of Organic Pollutants under Visible Light. *Nano* **2019**, *14* (11). https://doi.org/10.1142/S1793292019501364/ASSET/IMAGES/LARGE/S1793292019501364.JPEG.

(10) Ali, A.; Shoeb, M.; Li, Y.; Li, B.; Khan, M. A. Enhanced Photocatalytic Degradation of Antibiotic Drug and Dye Pollutants by Graphene-Ordered Mesoporous Silica (SBA 15)/TiO2 Nanocomposite under Visible-Light Irradiation. *J Mol Liq* **2021**, *324*, 114696. https://doi.org/10.1016/J.MOLLIQ.2020.114696.